

Sousa H.S., Branco J.M., Lourenço P.B., Neves L.C. (2016). Inference of stiffness and strength of chestnut timber members by use of Hierarchical Bayesian Probabilistic Networks, *Materials and Structures* 49(10). pp 4013-4028 (doi.org/10.1617/s11527-015-0770-8)

The final publication is available at [link.springer.com](http://link.springer.com):  
<http://link.springer.com/article/10.1617/s11527-015-0770-8>

# **Inference on stiffness and strength of existing chestnut timber elements using Hierarchical Bayesian Probability Networks**

Hélder S. Sousa <sup>a\*</sup>, Jorge M. Branco <sup>a</sup>, Paulo B. Lourenço <sup>a</sup>, Luís C. Neves <sup>b</sup>

<sup>a</sup> *Department of Civil Engineering, ISISE, University of Minho, Portugal*

<sup>b</sup> *Faculty of Engineering, NTEC, University of Nottingham, United Kingdom; Universidade Nova de Lisboa, UNIC, Portugal*

<sup>\*</sup> *corresponding author: ISISE, University of Minho*

*Department of Civil Engineering, Azurém,*

*4800-058 Guimarães, Portugal*

e-mail: [sousa.hms@gmail.com](mailto:sousa.hms@gmail.com)

Tel: +351 253510200; Fax: +351 253510217

e-mail addresses: Hélder S. Sousa - [sousa.hms@gmail.com](mailto:sousa.hms@gmail.com)

Jorge M. Branco - [jbranco@civil.uminho.pt](mailto:jbranco@civil.uminho.pt)

Paulo B. Lourenço - [pbl@civil.uminho.pt](mailto:pbl@civil.uminho.pt)

Luís C. Neves - [luis.neves@nottingham.ac.uk](mailto:luis.neves@nottingham.ac.uk)

## Abstract

The assessment of the mechanical properties of existing timber elements could benefit from the use of probabilistic information gathered at different scales. In this work, Bayesian Probabilistic Networks are used to hierarchically model the results of a multi-scale experimental campaign, using different sources of information (visual and mechanical grading) and different sample size scales to infer on the strength and modulus of elasticity in bending of structural timber elements.

Bayesian networks are proposed for different properties and calibrated using a large set of experimental tests carried out on old chestnut (*Castanea sativa* Mill.) timber elements, recovered from an early 20<sup>th</sup> century building.

The obtained results show the significant impact of visual grading and stiffness evaluation at different scales on the prediction of timber members' properties. These results are used in the reliability analysis of a simple timber structure, clearly showing the advantages of a systematic approach that involves the combination of different sources of information on the safety assessment of existing timber structures.

## Keywords:

*Structural reliability; Bayesian Probabilistic Networks; Existing timber structures; Bending stiffness; Bending strength*

# 1. Introduction

The assessment of existing timber structures is often a complex engineering procedure, given the variability of the material and the existing deterioration. Within each level of assessment, data deriving from different sources and analysis must be categorized by distinct importance, and dependency relations must be defined. This need arises even at material level where wood species, origin, growth characteristics, presence of defects among others, have an important influence on the mechanical performance of the material and thus of the structural member.

Mechanical properties of timber are often derived by empirical relations, from the so-called reference properties. These key properties are the modulus of elasticity (MOE) in bending, the bending strength ( $f_m$ ) and the density ( $\rho$ ). Correlations among these properties and with other mechanical properties are commonly found in literature (JCSS, 2006). In addition, several works address the correlation of these properties with non-destructive tests (NDT) (Cavalli and Togni, 2013; Bonamini et al., 1995; Feio and Machado, 2015; Faggiano et al., 2011; Sousa et al. 2013b; Calderoni et al., 2010; Bertolini et al. 1998). As mentioned by Vega et al. (2012), many works demonstrate the adequacy of NDT, such as acousto-ultrasonic tests, visual grading, knot diameter ratios and other indirect methods like machine grading to estimate bending MOE and density. In Cavalli and Togni (2013), old timber members were visually graded and tested with different nondestructive techniques for the density and MOE estimation. However, the prediction of bending strength, which is influenced by the visual grading parameters of timber, is less well defined. As mentioned by Isaksson (1999), the grading parameters are fundamental factors when choosing how and where to test a timber element. In that scope, different models have been considered to simulate the interrelation between quantitative knot indicators and strength parameters (Isaksson, 1999; Denzler, 2007). In Fink et al. (2011) the interrelation between bending

and/or tensile strength for different knot indicators have been discussed. Moreover, bending and tensile strength was also predicted regarding their morphological characteristics according to knot sections and clear wood sections (Fink et al, 2014).

In existing timber elements, the duration of load is an important parameter for the quantification of bending strength as noted by Madsen (1992), and this phenomena has also been modelled analytically and in a probabilistic perspective (Barrett and Foschi, 1978; Gerhards, 1979) by the consideration of damage accumulation models.

Concerning distinct sources of information and the variability of the reference properties within a structural member, which influence the correlation to other mechanical properties of timber, it is useful to hierarchically model the problem by defining the different situations or characteristics that allow inference on the target result. Such a hierarchical approach may be beneficial as a mean to provide information about a complex structural system by knowledge obtained solely from information of the material and element scales, and their relation to the system. In this context, Deublein et al. (2011) considered the use of Bayesian Probabilistic Networks (BPNs) to describe the influence of different origins, or dimensions, of sawn structural timber, on relevant timber material properties with additional evidences provided by measurements from a grading machine process.

The present work addresses the mechanical characterization of structural size elements using information of bending tests and visual inspection in twenty old chestnut (*Castanea sativa* Mill.) floor beams, collected from an early twentieth century building. The information gathered in the experimental campaign is hierarchically modeled using BPNs, accounting for different sources of information (visual and mechanical grading) and different size scales. The objective is to infer on chestnut timber mechanical properties, namely bending stiffness and strength, based on the visual and mechanical grading of smaller size scale specimens, using a probabilistic framework. Furthermore, the proposed model allows updating the timber elements' mechanical properties based on new information. The

influence of duration of load was not considered in the present work, to avoid the implementation of further uncertainty, as the objective was to combine information between visual grading with the information of bending tests. This framework is applied in a safety assessment example contemplating different prior information and the updated results retrieved from the BPN.

## **2. Framework for data analysis**

### **2.1. Experimental campaign data**

Aiming at assessing the bending stiffness and strength of structural size elements by use of visual inspection and local measurements, twenty chestnut (*Castanea sativa* Mill.) beams were visually graded and the results were compared to 4-point bending test results. The experimental methodology consisted in testing a full scale element (beam), then cutting it into smaller specimens (boards) and retesting them, in order to isolate the influence and location of defects, and also to provide a better definition of the distribution of stiffness and strength along the length and height of the beam. The main results and correlations between testing phases of the experimental campaign and analysis of variation of bending stiffness are presented in Sousa et al. (2015). The two experimental phases correspond to the elements dimensions: (i) sawn beams with  $7 \times 15 \times 300 \text{ cm}^3$ ; and (ii) sawn boards with  $7 \times 4 \times 300 \text{ cm}^3$  taken from the previous beams. A total of sixteen beams were sawn to boards (Figure 1), while four beams were tested up to failure for determination of bending strength. In each phase, the elements were visually inspected and graded in 40 cm segments according to UNI 11119 (2004). This standard establishes objectives, procedures and requirements for the diagnosis of the state of conservation, and estimates nominal stiffness and strength values for timber members in historical timber structures. Due to its applicability for onsite

measurements and since it provides information about the wood species of the elements analyzed in this work, this standard was considered hereafter. For strength grading of a single element, the standard considers three classes (I, II and III) regarding on-site diagnosis. The wood element is classified in a given class if it fulfills all the imposed requirements. Otherwise, it is graded in this study as non-classifiable (NC). UNI 11119 (2004) defines a method for grading elements focusing on the critical region of each element which is considered when the presence of defects, position, conservation state and/or loading state obtained through a static analysis are relevant for the aim of the diagnosis process. In spite of this premise, in this study all segments were considered for visual grading, in order to provide a larger size sample with broader variety of defects. Therefore, results of visual grading were obtained at segment and element level. The relationship between visual grading ( $VI$ ) in different size scales (beam and board) for the adopted sample is shown in Figure 2. These results show a significant correlation between grading at different scales, in particular for classes I and NC. In this case, a higher percentage of boards with  $VI_{\text{board}} = \text{I}$  is found for beams with  $VI_{\text{beam}} = \text{II}$ , decreasing progressively as the visual grading in the beams decreases. The higher percentage of segments with  $VI_{\text{board}} = \text{NC}$  is found for beams with  $VI_{\text{beam}} = \text{NC}$ . Although lower, correlation between visual grading in the different scales is also visible for class II. In the grading procedure, class I is only assigned if all segments are in good condition, whereas grading II and III can be assigned to more heterogeneous beams. As a result, intermediate grades (I and III) present less evident correlation between grades compared to the extreme grades (I and NC). Further detail on the effectiveness and subjectivity of visual inspection in chestnut elements can be found in Sousa et al. (2013a).

The sawn beams and boards were also submitted to 4-point bending test according to EN 408 (CEN, 2010), and the local ( $E_L$ ) and global ( $E_G$ ) modulus of elasticity in bending and bending strength ( $f_m$ ) were obtained. The results of the bending tests regarding stiffness and strength parameters are compiled in Table 1. Usually the value of  $E_G$  is lower than  $E_L$  due to

the contribution of the shear deformation, however some works have attained different results (Solli, 2000; Faggiano et al., 2011). In this work,  $E_{G,beam}$  was slightly higher than the value of  $E_{L,beam}$  (less than 1% on average). This difference might have resulted from errors occurring due to a slight initial twist of the elements and also because the  $E_{L,beam}$  was not necessarily tested in the most critical segment, as the objective was to test the element in the conditions that would be more similar to the onsite conditions. It must be noted that the sample size considered for the determination of bending stiffness and strength of beams is small (20 and 4, respectively), limiting the conclusions that can be drawn from the results.

In order to quantify the influence of visual grading on bending parameters, the results are detailed by visual class, evidencing a decrease of mean value and increase of variability from higher to lower grades. It is also clear from Table 1 that the bending strength is considerably affected by the size of the specimen, as a consequence of the inelastic behaviour of timber in presence of defects. The dimensions of a timber element affect the bending strength (size effect), since the probability of having weaker regions increases with the element dimensions. The differences between mean values of bending strength for beams and boards are large. This results from the small sample size of beams and the fact that only class II and NC beams were available. This presents significant heterogeneity, resulting in a significant number of class I segments (almost 50% of the full sample for boards). When considering the same class, the differences are less significant.

## **2.2. Bayesian Probabilistic Networks**

A Bayesian Probabilistic Network (BPN) is a probabilistic modeling method which allows a consistent and robust reasoning within a complex system with uncertain knowledge. BPNs are used to represent knowledge on a system based on Bayesian regression analysis, describing the causal interrelationships and the logical arrangement of the network variables. BPNs provide a causal and graphical mapping representation of the system properties and

features, as they explicitly define the dependency among variables (see e.g. Pearl (1988) and Jensen (2001) for a general introduction and Aguilera et al. (2011) and Weber et al. (2012) for advantages and disadvantages of these methods compared with other methods).

The common representation of a BPN consists in a directed acyclic graph (DAG), composed by a set of nodes, representing each system variable, connected by a set of directed edges, linking the variables in terms of their dependency or cause-effect relationship. The causal relationship structure of a BPN differentiates child node variables with ingoing edges (effects), from parent node variables with outgoing edges (causes). The direction-dependent criterion of connectivity, called *d-separation*, evidences the induced dependency relationship among variables and according to different arrangements are defined as converging, diverging or serial (or cascade) (Pearl, 1988). Each variable node represents a random variable, which is either defined as a continuous random variable or as a finite set of mutually exclusive discrete states. The main objective of a BPN is to calculate the distribution probabilities regarding a certain target variable, by carrying out the variables' joint distribution factorization based on the conditional interrelationships within a generic algorithm developed for that purpose. In this context, the DAG is the qualitative part of a BPN, whereas the conditional probability functions serve as the quantitative part. When discrete states are used, each random variable is defined by conditional probability tables, with the exception of nodes without parents which are defined by their marginal probabilities.

In the present work, a hierarchical BPN is initially used to infer on MOE in bending using mechanical properties and visual inspection grading at different scales (Figure 3). Results of visual inspections are classified in 4 classes (I, II, III and NC) according to UNI 11119 (2004), as discussed above. As shown in Sousa et al. (2015), a significant dependence exists, for the samples under analysis, between the bending MOE and the visual strength grading.



Consequently, visual inspection grading is used herein as an indicator to distinguish segments with different bending MOE results for the representation of the BPNs.

The purpose of this BPN is to infer on the global stiffness in bending of structural size beams,  $E_{G,beam}$ , by prior localized information on smaller size scale elements. To that aim, both boards' visual inspection grading,  $VI_{board}$ , and local MOE in bending,  $E_{L,board}$ , are considered as parent nodes. In this BPN, the parent nodes in a smaller scale (board scale) are representative of the results obtained for the local segments that compose the structural element (beam scale). In terms of visual inspection, the grading of the element is related to the grading of the critical segment (local information on the board scale) and, therefore, their cause-effect relation. In terms of bending modulus of elasticity, the global value is directly affected by the variation of stiffness along the element. In order to infer on the global modulus of elasticity, the information of both local modulus of elasticity of the segments and visual inspection, are considered in parallel.

After inferring on MOE in bending, a BPN for inferring on the bending strength,  $f_m$ , was considered. This BPN takes into consideration that timber failures are more prone to take place in weak sections corresponding to sections with significant defects (or their neighboring sections), and therefore  $f_m$  is analyzed at a small size scale regarding the visual grading of the boards segments. Also in Czomch et al. (1991), Isaksson (1999) and Köhler (2007), the within member variability of strength was studied regarding the subdivision of the timber members in sections with or without major knots and knot clusters. Although the mentioned literature used segments of varying width, to emulate the growth characteristics, in this work, the objective is to define methods to assess the properties of sawn timber beams rather than relate the properties with growth. Consequently, geometries closer to commercial dimensions were used. Segments length was also obtained considering that visual inspection standards often consider the analysis of critical segments.

The states in  $VI_{\text{board}}$  correspond to the different visual grades (I, II, III and NC), whereas the states of  $E_{G,\text{board}}$  are considered by intervals of  $2500 \text{ N/mm}^2$  up to  $17500 \text{ N/mm}^2$ , with an initial interval of  $[0,5000[ \text{ N/mm}^2$  so as to prevent an interval without any event. Intervals of  $10 \text{ N/mm}^2$ , starting from 0 and up to  $90 \text{ N/mm}^2$  are considered for the discrete representation of the child node  $f_{m,\text{board}}$ . The interval size for  $E_{G,\text{board}}$  ( $2500 \text{ N/mm}^2$ ) and for  $E_{L,\text{board}}$  ( $2000 \text{ N/mm}^2$ ) are different as to attend to a more uniform distribution of values within intervals and to maximize the number of combinations between parent and child nodes with significant number of events. In this experimental campaign the global MOE in bending,  $E_{G,\text{board}}$ , resulted in a better correlation with the bending strength,  $f_{m,\text{board}}$ , compared to the local MOE in bending,  $E_{L,\text{board}}$ , with a higher coefficient of determination  $r^2$  ( $0.69 > 0.38$ ). As the  $E_{G,\text{board}}$  provided a better fit to the existing data sample, it was chosen as a parent node. The arrangement of the parent nodes was conditioned by the available data results and expert decision. As insufficient data regarding the bending strength of beams was available for the validation of a BPN, only the results of the tests in boards were considered. Also in this experimental campaign, segments that were given higher visual grading (I and II classes) and evidenced high values of  $E_{G,\text{board}}$ , did not produce any event with low value of  $f_{m,\text{board}}$ . On the other hand, segments that were given lower visual grading (III and NC classes) and evidenced low values of  $E_{G,\text{board}}$ , did not produce any event with high value of  $f_{m,\text{board}}$ . Therefore, in a discrete BPN, this prior information cannot be described by two converging nodes, as the conditional probability tables for the child node would evidence non-existing events. To prevent this situation, a series BPN was considered having, as first parent node, the  $VI_{\text{board}}$  followed by the  $E_{G,\text{board}}$  (Figure 4). The objective of this network is to infer on the localized bending strength of a section, based on its visual inspection grading and bending stiffness. This is also useful for the assessment of the structural size element since, as mentioned before, the failure of the global element is often associated to a specific weak section.

In both BPNs, the relations between nodes were made considering the inference of a reference property. Visual grading was only directly connected to the modulus of elasticity when the same scale was considered to the reference property in analysis.

In the present work, the inference engine from (Hugin, 2008) was applied to build the network and to calculate the marginal probability values for the BPNs inferring on bending stiffness and strength.

### 3. Results

The results are provided regarding the inference process made within each considered BPN. Each BPN is identified regarding the final child node. In the first BPN, emphasis is given for the inference on  $E_{G,beam}$  which corresponds to its last child node. The second BPN focus on the inference on  $f_{m,board}$ , as it is its last child node, however the results of the intermediate node regarding  $E_{G,board}$  are also presented to establish a better comparison basis between BPNs.

#### 3.1. Bending Modulus of Elasticity

In the following, the results respecting the inference stage of the BPN for the hierarchical modeling of MOE, during which different prior evidence in form of knowledge upon the states of the parent nodes is entered in the model, are presented. For that purpose, the probabilities within the BPN are updated through Bayes' theorem regarding the belief propagation within the arrangements of nodes of the different networks. The results are provided regarding the inference on MOE by use of the network in Figure 3, and are considered in terms of cumulative frequency of the posterior updated probabilities tables of the respective discrete functions. In Figures 5 and 6, the probability distributions of the beam MOE are shown, considering the experimental results with no evidence, or combining

this data with visual inspections and board MOE. Figure 5 shows the results obtained using, as input, the visual grading of the beam while, for results in Figure 6, the input considered was the result of visual grading on the board. Figure 5 allows the analysis of the importance of entering information regarding smaller size specimens in the definition of the mechanical properties of structural size members, not only when a given  $VI_{\text{beam}}$  is considered but also between different  $VI_{\text{beam}}$ . On the other hand, Figure 6 considers the combination of information regarding only the smaller scale specimens by evidence in  $VI_{\text{board}}$  and  $E_{L,\text{board}}$ , allowing for the assessment of the evolution of  $E_{G,\text{beam}}$  based in the variation of that evidence.

The results show a clear dependence between the result of visual grading and the beam MOE. As shown in Figure 5.a, beams classified as grade II result in significantly higher beam MOE, while for grade NC (Figure 5.c) a reduction in beam MOE is observable. Class II beams present posterior distributions with higher values of  $E_{G,\text{beam}}$  than the prior distribution. For these beams, cumulative frequency above 10% are only found for values of  $E_{G,\text{beam}}$  higher than  $13000 \text{ N/mm}^2$ , independently of the evidence in  $E_{L,\text{board}}$ . Lowering the  $VI_{\text{beam}}$  to class III produces posterior frequency distributions around the range of the prior distribution without evidence in  $E_{L,\text{board}}$ , whereas lowering the  $VI_{\text{beam}}$  to class NC produces posterior distributions with lower values of  $E_{G,\text{beam}}$  than the prior distribution without evidence in  $E_{L,\text{board}}$ . Exception to these defined ranges are found when  $VI_{\text{beam}} = \text{NC}$  and  $E_{L,\text{board}} > 17000 \text{ N/mm}^2$ , where the posterior distributions still present higher values of  $E_{G,\text{beam}}$  than the prior distribution, at the lower tail of the distributions and almost until 50% of cumulative frequency, evidencing that information about  $E_{L,\text{board}}$  is relevant in the infer on  $E_{G,\text{beam}}$  at this hierarchical BPN. In Figure 5, an overall positive correlation is found between the different intervals of modulus of elasticity, meaning that a higher evidence for  $E_{L,\text{board}}$  leads to higher values of  $E_{G,\text{beam}}$ . However, due to the empirical nature of the input variables,

and when a low number of events exists, it is possible to find cases where this positive correlation is not found (e.g.  $E_{G,beam} \mid VI_{beam}=III \cap E_{L,board} > 19 \text{ N/mm}^2$ ).

The relevance of  $E_{L,board}$  is further highlighted in Figure 6, where it is shown that values of  $E_{L,board}$  lower than  $11000 \text{ N/mm}^2$  produces lower values of  $E_{G,beam}$  than the prior distribution, whereas, values of  $E_{L,board}$  above  $15000 \text{ N/mm}^2$  produce higher values of  $E_{G,beam}$  in the lower tail considering all possible evidence in  $VI_{board}$ . For evidences in  $E_{L,board}$  ranging from  $11000$  to  $15000 \text{ N/mm}^2$  the posterior distribution are similar to the prior distribution without evidence in  $E_{L,board}$ .

When taking small specimens from a structural member for mechanical characterization, often clear wood samples are adopted for reference values as they present less variability than specimens with defects. Moreover, clear wood specimens also present advantages regarding an easier cutting process and preparation for testing (Brites et al., 2012; Kloiber et al., 2015). Clear wood specimens presenting no visible defects are graded as class I. Although minor defects are acceptable in class I, these defects must be considered as not affecting significantly the element in a structural scale. In this work, and considering the same network for the assessment at a structural scale, clear wood specimens are classified as visual grade I. As previously mentioned, in accordance to normal practice when assessing a timber element onsite, information is made available for clear wood specimens. Using this BPN for the use of an existing timber element, the results of the inference on the posterior probability of  $E_{G,beam}$  is presented when evidence is given such that  $VI_{board} = 1$  (simulating information provided by segments of clear wood) combined with different evidences given for the node of  $E_{L,board}$ . The results are given in Figure 7. For the case of  $VI_{board} = I$ , a clear trend for higher values of  $E_{G,beam}$  is found when increasing the values in the evidence of  $E_{L,board}$ . When comparing with the prior distribution with no evidence in  $E_{L,board}$ , posterior distributions with lower values of  $E_{G,beam}$  are found when evidence in  $E_{L,board}$  indicates

values lower than  $11000 \text{ N/mm}^2$ , while evidence indicating  $E_{L,board}$  higher than  $11000 \text{ N/mm}^2$  infers on posterior distributions with higher  $E_{G,beam}$  values than the prior distribution. In general, a decrease in mean and characteristic values is found for lower visual grading classes, whereas an increase with the MOE of boards is observed. Results deriving from a combination of evidences with a low number of events (less than 3 events) should be disregarded, as they may not be representative of the actual properties of existing timber elements.

The effect of the beam and board visual grading on the computed mean  $E_{G,beam}$  showed significant differences across classes. When assuming the same  $E_{L,board}$  class, the mean value of  $E_{G,beam}$  significantly changes between different visual grading classes. When considering evidence in the BPN regarding the visual grading ( $VI_{beam} = \text{II, III or NC}$ ), an average difference between results with different visual grades is 2.5%, whereas when visual grading is known for the board scale ( $VI_{board} = \text{I, II, III or NC}$ ) this difference increases to 15.1%. Comparing these values, it is observed that the difference is significantly higher for the case of evidence in visual grading in boards. This is consequence of the visual grading process where, for the case of beams, the global grading is given considering the critical segment. This means that similar beams may have different grades if having a different critical segment grading, whereas the grading in boards, due to the smaller scale size, allows for a better differentiation between classes.

On the other hand, when fixing the same visual grade but analyzing the value of  $E_{G,beam}$ , accounting for different evidences given to the class of  $E_{L,board}$ , an average difference of 2.9% and 2.5% are found, for visual grade evidence given on  $VI_{beam}$  or  $VI_{board}$ , respectively, between consecutive  $E_{L,board}$  classes. Difference values are low due to the relatively small interval between  $E_{L,board}$  classes ( $2000 \text{ kN/mm}^2$ ).

These results clearly show that worst grading implies lower mean  $E_{G,beam}$ . Excluding the combination of evidences with low number of events, the results of beam grading show

differences in the mean  $E_{G,beam}$  of up to 26.7% between grading classes, considering the same mean  $E_{L,board}$ . The impact of local grading ( $VI_{board}$ ) is smaller, but still significant, with differences between classes of up to 19.3% when a similar  $E_{L,board}$  is considered. Also excluding the combination of evidences with low number of events, for a board classified as class I, different values of consecutive intervals of  $E_{L,board}$  result in differences of up to 6.0% in the  $E_{G,beam}$ . Similar values are found for other grading classes in most of the combination of evidences.

### 3.2. Bending Strength

The results of the proposed series BPN for inference on the bending strength of boards,  $f_{m,board}$ , regarding the posterior probabilities expressed by histograms of the distribution frequency curves, are presented in Figure 8, with evidence entered at the parent node  $VI_{board}$  (Lognormal distributions were adjusted regarding the statistical parameters of the posterior probabilities histogram). The propagation of evidence through the BPN allows to infer on the  $E_{G,board}$  and  $f_{m,board}$ . In both cases, a clear distinction is found between the obtained probability density function with  $VI_{board}$  evidence, indicating higher mean values and lower variability for the mechanical properties as the visual grade increases. The exception is the value of coefficient of variation for  $E_{G,board}$  when evidence is given as  $VI_{board} = I$ . In that case, the variability is higher than for lower classes ( $VI_{board} = II$ ) because the grading process considers that segments without any defect are classified as class I, but also admits segments with minor defects, therefore the interval of the grading parameters is higher.

By comparison with the prior distribution curve ( $VI_{board} = \text{no evidence}$ ), in the case of inference on  $E_{G,board}$  similar values are obtained when  $VI_{board} = III$  is considered, while in the case of inferring on  $f_{m,board}$ , similar values are found with  $VI_{board} = II$ . This is consequence of the selection process made for the segments that were considered for the bending strength tests, where more segments with higher classes were considered. Therefore, when no

evidence is provided the results of bending strength are more influenced by the higher grade segments results as they represent a larger number within the sample considering all results. These results are also consistent with the consideration that clear wood has a higher influence on stiffness as it is mostly determined by average properties rather than by local weak sections, whereas bending strength depends mainly on the variation of the material properties and local defects (Piazza and Riggio, 2008).

The statistical parameters of the posterior distributions, with evidence in  $VI_{\text{board}}$ , are presented in Table 2. Mean and CoV were determined based on the posterior probability histograms, while the characteristic values (corresponding to the 5<sup>th</sup> percentile) were derived considering the distribution curves provided in Figure 8. In all cases, a decrease of the mean and characteristic values is found when lowering the visual inspection grade. The average difference between mean values of consecutive grading classes is 25.2% and of 19.5%, for inference on  $E_{G,\text{board}}$  and  $f_{m,\text{board}}$ , respectively. Higher decrease in the mechanical properties is found when lowering from class III to class NC (40.6% and 31.9%, respectively for  $E_{G,\text{board}}$  and  $f_{m,\text{board}}$ ).

Within the scope of the European norm EN 338 (CEN, 2009) strength class system, the importance of the BPN inferring on both  $E_{G,\text{board}}$  and  $f_{m,\text{board}}$  is noticeable when evidence is given on  $VI_{\text{board}}$ . In this case, and assuming the statistical results of the underlying probabilistic distribution for the bending stiffness and strength, a D24 class is attributed when no evidence is given to visual grading. An increase in strength class to D30 or D40 is present, respectively, when  $VI_{\text{board}} = \text{II}$  or  $VI_{\text{board}} = \text{I}$ . On the other hand, a decrease to strength class D18 is present when  $VI_{\text{board}} = \text{III}$  and no strength class is admitted for  $VI_{\text{board}} = \text{NC}$  since the required values are not fulfilled.



## 4. Reliability analysis

Safety assessment of an existing structure requires that the actual mechanical properties of the structural elements are evaluated regarding the relevant failure modes. For that aim, limit state functions are considered to represent the realizations of the resistance parameters with updated information on the material properties and loading conditions. In timber structures, the probabilistic modeling of the mechanical properties is of special interest due to the different sources of uncertainty inherent to the material. In this case study, the results derived from the BPNs inference are used in a reliability assessment of a simple structure. The example consists of a simply supported solid timber beam, with rectangular cross section, with height  $h$  and width  $b$ . The loads (permanent and variable) are assumed uniformly distributed along the beam length,  $l$ . The permanent load is defined by a Normal distribution with 3.0 N/mm mean and  $\text{CoV} = 0.10$  (JCSS, 2001), and the live load is defined by a Gumbel distribution with 2.0 N/mm mean and  $\text{CoV} = 0.40$  (Ranta-Maunus, 2004). Bending strength and stiffness are defined by Lognormal distributions with statistical parameters given by the output of the BPN. More information about basic principles of structural reliability and of reliability based code design may be found in Faber and Sørensen (2002), Hansen and Sørensen (2002) and Köhler and Fink (2012).

As the interest of this work resides in inference on the mechanical properties of existing timber elements, the cross section dimensions were defined as deterministic parameters. The width is fixed to a value of 200 mm, while the height is calculated such that it provides an appropriate value of design for the case where no information is given on the bending mechanical properties of the element.

In a reliability analysis, model uncertainties should be considered regarding deviations and simplifications related to the probabilistic parameter modelling and to the considered limit state equations. Commonly, reference properties are obtained through standardized tests,

whereas estimation of other materials parameters based on those reference properties should include model uncertainties. Moreover, both load and resistance models present uncertainty which can be modelled as random variables (JCSS, 2006; Köhler and Fink, 2012). In the present work, model uncertainties regarding the limit state equations were not included, aiming at considering directly the results of the tests on the reference properties as to apply them in an example for comparison basis when different evidences were provided within a BPN.

#### 4.1. Ultimate limit state verification

Initially, the mechanical properties are provided given the mean and coefficient of variation of the posterior probability distribution resulting from the inference within the BPN without any prior evidence. In a first step, the results deriving from the BPN that infers on bending strength,  $f_m$  (see Table 2), are applied.

For the reliability verification of structures, limit state equations are required, which in this study were defined with reference to EN 1995-1-1:2004 (CEN, 2004) with the necessary changes for a probabilistic analysis. The modification parameter regarding the effect of load duration and moisture content of timber,  $k_{mod}$ , is considered for the load with smaller duration. In this case, the limit state equation  $g$  is given by Equation (1).

$$g = \frac{1}{6}bh^2k_{mod}f_m - \frac{1}{8}l^2(G + Q) \quad (1)$$

In this case, the resistance of the global member (beam scale) was considered to be equal to the resistance of the critical section (board scale), thus information is considered to be retrieved and representative of that critical section. Considering a height of 300 mm, a reliability index,  $\beta$ , of 4.70 is obtained. Following the same structural conditions and loading scenario, different levels of information were introduced to the parent node regarding visual grading in the lower size scale. The reliability indices obtained considering different

outcomes of a visual grading are presented in Figure 9. When information is given as  $VI_{\text{board}} = \text{I}$ , the reliability index is higher than the one obtained with no prior evidence, whereas for  $VI_{\text{board}} = \text{III}$  or  $VI_{\text{board}} = \text{NC}$  the reliability index is lower. The consideration of  $VI_{\text{board}} = \text{II}$  led to similar reliability index compared with the case of no prior evidence.

For the case of  $VI_{\text{board}} = \text{III}$  or  $\text{NC}$ , the introduction of new information resulted in unsatisfactory levels of structural safety ( $\beta < 4.2$ ). The case of  $VI_{\text{board}} = \text{NC}$  results in a high decrease compared to the visual grade immediately before (class III), showing an unsafe structural level. This is mainly due to the large variation found in that class combined with a lower mean value of bending strength.

The influence of different levels of information is also assessed in terms of design value by determining the cross section height, for each case with evidence, which would provide the same reliability level of the case with no evidence. In this example, when having  $VI_{\text{board}} = \text{I}$ , a 15.7% smaller height would provide a  $\beta = 4.70$ , whereas the other cases would need an increase of height to provide the same reliability index. These increases would be of 1.0%, 21.7% and 132.7% for  $VI_{\text{board}} = \text{II}$ ,  $VI_{\text{board}} = \text{III}$  and  $VI_{\text{board}} = \text{NC}$ , respectively.

## 4.2. Serviceability limit state verification

After assessing the safety level regarding the ultimate limit state, the results derived from the hierarchical BPN that infers on bending stiffness are applied considering the loading scenario and span between supports equal to the previous example. However, in this case, the deflection for the serviceability limit state is assessed. For structures consisting of members, components and connections with the same creep behaviour and under the assumption of a linear relationship between the actions and the corresponding deformations, the final deformation may be taken as the sum of the effect of each action considered separately (CEN, 2004). Each component of deflection is then affected by the stiffness

modification factor,  $k_{\text{def}}$ , according to the service class, and by the factor for quasi-permanent value for variable loads,  $\psi_2$ .

The component of deflection for permanent load,  $u_G$ , was obtained through Equation (2) and the component for variable load,  $u_Q$ , was obtained through Equation (3).

$$u_G = \left( \frac{5}{384} \cdot \frac{G \cdot l^4}{E \cdot b \cdot h^3 / 12} \right) \cdot (1 + k_{\text{def}}) \quad (2)$$

$$u_Q = \left( \frac{5}{384} \cdot \frac{Q \cdot l^4}{E \cdot b \cdot h^3 / 12} \right) \cdot (1 + \Psi_2 \cdot k_{\text{def}}) \quad (3)$$

Here,  $E$  is the bending modulus of elasticity,  $G$  is the permanent load and  $Q$  is the variable load as considered in the previous example,  $b$  and  $h$  are the cross section width and height, respectively,  $k_{\text{def}}$  is the stiffness modification factor and  $\psi_2$  is the factor for quasi-permanent value for the live load. Considering that the structure is in a residential building, and is built of solid timber in a service class 1 environment, the values of  $k_{\text{def}} = 0.6$  and  $\psi_2 = 0.3$  are attained (CEN, 2002 and 2004).

The deflection of the beam is assessed for the central section by considering the serviceability limit state equation  $g$  as:

$$g = \delta_L - (u_G + u_Q) \quad (4)$$

where  $\delta_L$  is the allowable deflection limit dependant of the span length (in this case  $\delta_L = l/350$  was adopted).

A height equal to 435 mm was considered, obtaining a  $\beta = 2.92$  (reference period of one year) when no evidence is given in the BPN. This reliability level is consistent with the indication of Annex C of CEN (2002) for reliability class 2. Comparing to the ultimate state verification, it is found that the serviceability limit state is the most conditioning in terms of cross section height.

Following the same structural conditions and loading scenario, different levels of information were introduced to the parent nodes regarding visual inspection grading in different size scales and information of  $E_L$  in the board scale. The results evidence that lower reliability indices are found when evidence indicates lower visual grading and lower values of  $E_{L,board}$  and, on the opposite case, that higher reliability indices are found when evidence indicates higher visual grading ( $VI_{board} = I, II$  or  $VI_{beam} = II$ ) and higher values of  $E_{L,board}$  (Figure 10). Significant differences are found on the reliability indices between cases with different evidences in  $E_{L,board}$ .

Overall, according to the different combinations of evidence, the cross section height could be reduced up to 9.20% ( $VI_{beam} = II \cap E_{L,board} > 19 \text{ kN/mm}^2$ ) or would have to be increased 8.51% ( $VI_{beam} = NC \cap E_{L,board} < 5 \text{ kN/mm}^2$ ), as to obtain the same reliability index of the case when no evidence exists.

Although the relative differences in height are rather small for some cases, it is important to notice that these values may be comparable to the loss of cross section in existing timber structure exposed to decay. In that case, the combination of results of visual grading and local mechanical tests, combined through the proposed method, proves to be valuable in the verification of serviceability limit states for a decayed structure.

## 5. Concluding remarks

The implementation of grading procedures that allow for an explicit consideration of information during the grading process itself, and also for use in reliability assessment, is challenging when it concerns grading timber members of existing structures. However, many of the approaches reside within the same basic concept that the main properties of interest may be assessed indirectly by means of other properties.

The use of visual inspection of the structural element and information from small size specimens are common available data for the mechanical assessment of timber members. To that purpose, the previous described BPNs allowed to infer on bending stiffness and strength of timber members influenced by visual grading and mechanical tests made in different size scales. Given these influencing factors, the proposed BPNs were capable of updating the conditional probability distributions and showed that the marginal probability distributions of timber mechanical properties were significantly altered when provided different evidences. Clearly, more refined predictions of the mechanical properties can be obtained by increase of the states in either or both parenting and child nodes. Nevertheless, an increase of the refinement of states must be accompanied with a larger number of events (number of visual grading and mechanical test measurements) for a consistent and trustworthy assessment. Extension of the BPNs may be accomplished by adding nodes representing variables to which information is known or may become available, and after updating the interrelationships and probability distribution functions of those variables. These premises were implemented making possible to validate a BPN where the MOE of structural size timber members could be derived by information of mechanical test results made to small specimens combined with visual grading of the members at different size scales.

Moreover, the predicted marginal probability functions were used to determine the mean and characteristic values of the timber mechanical properties, consisting in an important step regarding the possible allocation of each sub-sample into a specific structural class, such as the system provided by EN 338 (CEN, 2009). In all cases of evidence in the visual inspection results of the board,  $VI_{\text{board}}$ , the limiting strength grading parameter was the mean MOE in bending. These results evidence that the use of BPN combined with multi-scale information on visual grading and mechanical testing provides a consistent basis for strength grading of existing timber members. Furthermore, this methodology may be applied to reliability assessment, as the uncertainty of each variable is passed throughout the

propagation of different evidences and reflected on the BPN results, as posterior marginal probability distributions. Further research may also address the implementation in a BPN of the influence of the location of each segment (board) on the global element (beam) as to assess the effect of the duration of load phenomena.

The results of the data inference on the BPNs were used in the verification of ultimate limit state in bending for a simply supported beam, and also for the deflection serviceability limit state. A comparison of the reliability indices considering different results of mechanical testing and visual inspections showed the importance of these results in the assessment of the structural safety.

The models and inference analysis addressed on this work were calibrated by the results obtained in a specific experimental campaign and are dependent on its sample size. Although the methodology may be adapted to different samples, further research with other wood species and larger number specimens, especially for the higher size scale, are needed for generalization of the results.

## Acknowledgments

The financial support of the Portuguese Science Foundation (Fundação de Ciência e Tecnologia, FCT), through PhD Grant SFRH/BD/62326/2009, is gratefully acknowledged. The authors acknowledge also the support of Augusto de Oliveira Ferreira e Ca., Lda. (offer of specimens).

## References

- Aguilera PA, Fernández A, Fernández R, Rumí R, Salmerón A (2011) Bayesian networks in environmental modelling. *Environ Modell Softw* 26(12):1376-1388. doi: 10.1016/j.envsoft.2011.06.004
- Barrett JD, Foschi RO (1978) Duration of load and probability of failure in wood. Part 1: modelling creep rupture. *Can J Civil Eng* 5(40):505-14

- Bertolini C, Brunetti M., Cavallero P, Macchioni N (1998) A non destructive diagnostic method on ancient timber structures: some practical application examples. In: WCTE98, 5th World Conference on Timber Engineering, Montreaux, Switzerland
- Bonamini G, Togni M, Uzielli L (1995) The strength and stiffness of large ancient timber beams: experimental assessment of the effectiveness of combined visual grading and non-destructive testing. In: 1st International Conference on Science and Technology for the Safeguard of Cultural Heritage in the Mediterranean Basin, Catania, Italy
- Brites RD, Lourenço PB, Machado JS (2012) A semi-destructive tension method for evaluating the strength and stiffness of clear wood zones of structural timber elements in-service. *Constr Build Mater* 34:136-144. doi:10.1016/j.conbuildmat.2012.02.041
- Calderoni C, De Matteis G, Giubileo C, Mazzolani FM (2010) Experimental correlations between destructive and non-destructive tests on ancient timber elements. *Eng Struct* 32(2):442-448
- Cavalli A, Togni M (2013) How to improve the on-site MOE assessment of old timber beams combining NDT and visual strength grading. *Nondestruct Test Eva* 28(3):252-262
- CEN (2002) EN 1990:2002, Eurocode 0: Basis of Structural Design, European Committee for Standardization, Brussels
- CEN (2004) EN 1995-1-1:2004, Eurocode 5: design of timber structures. Part 1-1: General common rules and rules for buildings, CEN European Committee for Standardization, Brussels
- CEN (2009) EN 338:2009. Structural timber - Strength classes. CEN European Committee for Standardization, Brussels
- CEN (2010) EN 408:2010 - Timber structures - Structural timber and glued laminated timber - Determination of some physical and mechanical properties, European Committee for Standardization, Brussels
- Czomch I, Thelandersson S, Larsen H (1991) Effect of within member variability on bending strength of structural timber. In: Proceedings of the CIB-W18 Meeting 24, Paper 24-6-3, Oxford, United Kingdom
- Denzler JK (2007) Modellierung des Größeneffektes bei biegebeanspruchtem Fichtenschnittholz. PhD dissertation, Technische Universität München, Germany
- Deublein M, Schlosser M, Faber MH (2011) Hierarchical modeling of structural timber material properties by means of Bayesian Probabilistic Networks. In: Faber, Köhler & Nishijima (eds) *Applications of Statistics and Probability in Civil Engineering*. Taylor & Francis Group, London. pp 1377-1385
- Faber MH, Sørensen JD (2003) Reliability based code calibration – the JCSS approach. In: ICASP9, vol. 2, pp. 927-935, San Francisco, USA



- Faggiano B, Grippa MR, Marzo A, Mazzolani FM (2011) Experimental study for non-destructive mechanical evaluation of ancient chestnut timber. *J Civ Struct Health Monitor* 1(3):103-112
- Feio A, Machado JS (2015) In-situ assessment of timber structural members: Combining information from visual strength grading and NDT/SDT methods - A review. *Const Build Mater*. doi:10.1016/j.conbuildmat.2015.05.123
- Fink G, Deublein M, Kohler J (2011) Assessment of different knot-indicators to predict strength and stiffness properties of timber boards. In: *Proceedings of the 44th Meeting, International Council for Research and Innovation in Building and Construction, Working Commission W18, Timber Structures*, Alghero, Italy, CIB-W18, Paper No. 44-5-1
- Fink G, Kohler J (2014) Model for the prediction of the tensile strength and tensile stiffness of knot clusters within structural timber. *Eur J Wood Wood Prod* 72(3):331-341. doi: 10.1007/s00107-014-0781-0
- Gerhards CC (1979) Time-related effects on wood strength: a linear cumulative damage theory. *Wood Sci* 11(3):139-44
- Hansen PF, Sørensen JD (2002) Reliability-based code calibration of partial safety factors. In: *Joint Committee of Structural Safety, JCCS-Workshop on Code calibration*.
- Hugin (2008) Hugin Researcher, Aalborg, Hugin Experts A/S
- Isaksson T (1999) Modelling the variability of bending strength in structural timber. Report TVBK-1015, Dept. of Structural Engineering, Lund University, Sweden
- JCSS (2001) JCSS Probabilistic Model Code, Part 2: Load Models. Probabilistic Model Code, Joint Committee on Structural Safety.
- JCSS (2006) JCSS Probabilistic Model Code, Part 3: Resistance Models – 3.5 Properties of Timber. Probabilistic Model Code. Joint Committee on Structural Safety
- Jensen FV (2001) *Bayesian Networks and Decision Graphs*. New York Springer
- Kloiber M, Drdácý M, Machado JS, Piazza M, Yamaguchi N. (2015, in press) Prediction of mechanical properties by means of semi-destructive methods: A review. *Constr Build Mater*. doi: 10.1016/j.conbuildmat.2015.05.134
- Köhler J (2007) Reliability of Timber Structures. PhD dissertation, Department of Civil, Environmental and Geomatic Engineering, Zurich, ETH Zurich
- Köhler J, Fink G (2012) Reliability Based Code Calibration of a Typical Eurocode 5 Design Equations. In: *WCTE 2012 conference*, vol. 4, pp. 99-103, Auckland, New Zealand.

- Madsen B (1992) Structural behaviour of timber, chapter 6: Duration of Load. Timber Engineering LTD, Canada. ISBN 0-9696162-0-1
- Pearl J (1988) Probabilistic Reasoning in Intelligent Systems: Networks of Plausible Inference. Morgan Kaufmann Pub.
- Piazza M, Riggio M (2008) Visual strength-grading and NDT of timber in traditional structures. *J Build Appraisal* 3(4):267-296
- Ranta-Maunu A (2004) Theoretical and practical aspects of the reliability analysis of timber structures. In: WCTE 2004 conference, Lahti, Finland.
- Solli KH (2000) Modulus of elasticity - local or global values. In: WCTE2000, 6th World Conference on Timber Engineering, Whistler, Canada
- Sousa HS, Branco JM, Lourenço PB (2013a) Effectiveness and subjectivity of visual inspection as a method to assess bending stiffness and strength of chestnut elements. *Adv Mat Materials Res* 778:175-182. doi: 10.4028/www.scientific.net/AMR.778.175
- Sousa HS, Sørensen JD, Kirkegaard PH, Branco JM, Lourenço PB (2013b) On the use of NDT data for reliability-based assessment of existing timber structures. *Eng Struct* 56:298-311. doi: 10.1016/j.engstruct.2013.05.014
- Sousa HS, Branco JM, Lourenço PB (2015) Use of bending tests and visual inspection for multi-scale experimental evaluation of chestnut timber beams stiffness. *J Civil Eng Manage.* doi: 10.3846/13923730.2014.914083
- UNI (2004) UNI 11119:2004 Cultural Heritage - Wooden artifacts - Load-bearing structures - On site inspections for the diagnosis of timber members. UNI Milano
- Vega A, Dieste A, Guaita M, Majada J, Baño V (2012) Modelling of the mechanical properties of *Castanea sativa* Mill. structural timber by a combination of non-destructive variables and visual grading parameters. *Eur J Wood Wood Prod* 70(6):839-844. doi: 10.1007/s00107-012-0626-7
- Weber P, Medina-Oliva G, Simon C, Iung B (2012) Overview on Bayesian networks applications for dependability, risk analysis and maintenance areas. *Eng Appl Artif Intel* 25(4):671-682. doi: 10.1016/j.engappai.2010.06.002

## List of Figures

**Fig. 1** Testing phases and specimen geometry.

**Fig. 2** Distribution of boards visual grading for beams with different visual grade, as: a) class II; b) class III; c) class NC.

**Fig. 3** Hierarchical BPN to infer on global MOE in bending of structural size members by prior localized information in smaller size elements.

**Fig. 4** Simplified converging model.

**Fig. 5** Cumulative frequency results for global MOE in bending for beams obtained with evidence in  $E_{L,board}$  results and beams' visual grade: a)  $VI_{beam} = II$ ; b)  $VI_{beam} = III$ ; c)  $VI_{beam} = NC$ . The markers indicate  $E_{L,board}$  results in  $kN/mm^2$ .

**Fig. 6** Evolution of cumulative frequency results with evidence in  $VI_{board}$ , throughout increasing of prior  $E_{L,board}$  (horizontal axes are  $E_{G,beam}$  in  $N/mm^2$  and vertical axes are frequency in %; the markers indicate  $E_{L,board}$  results in  $kN/mm^2$ ).

**Fig. 7** Cumulative frequency results for global MOE in bending for beams obtained with evidence in  $E_{L,board}$  results and for boards' visual grade I. The markers indicate  $E_{L,board}$  results in  $kN/mm^2$ .

**Fig. 8** Histogram results in board scale, obtained with different evidences in  $VI_{board}$ , for a)  $E_{G,board}$ ; b)  $f_{m,board}$ . The markers indicate the  $VI_{board}$ .

**Fig. 9** Reliability indices for different levels of prior information.

**Fig. 10** Reliability indices for different levels of prior information for the serviceability limit state with information in visual grade of: a) boards; b) beams.

## List of Tables

**Table 1** Mean and coefficient of variation (CoV) values for bending stiffness and strength obtained from sawn beams and boards

**Table 2** Mean and characteristic values for different evidences in the BPN for infer on  $f_{m,board}$

## Figures:

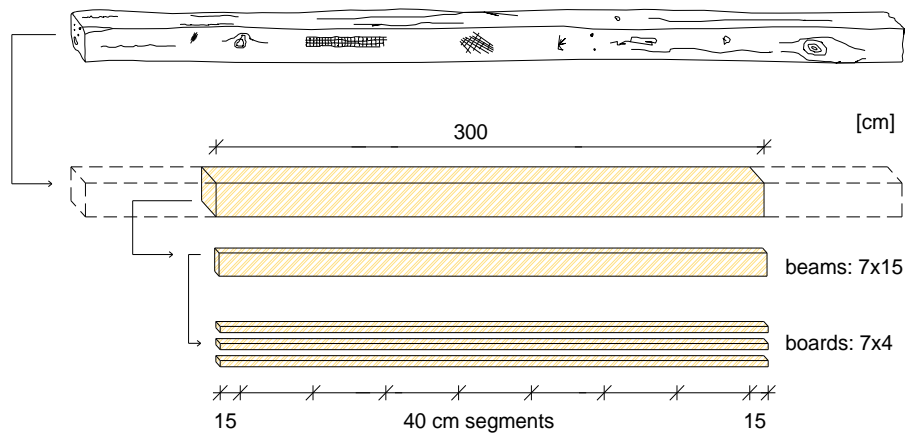


**Fig.1** Testing phases and specimen geometry.

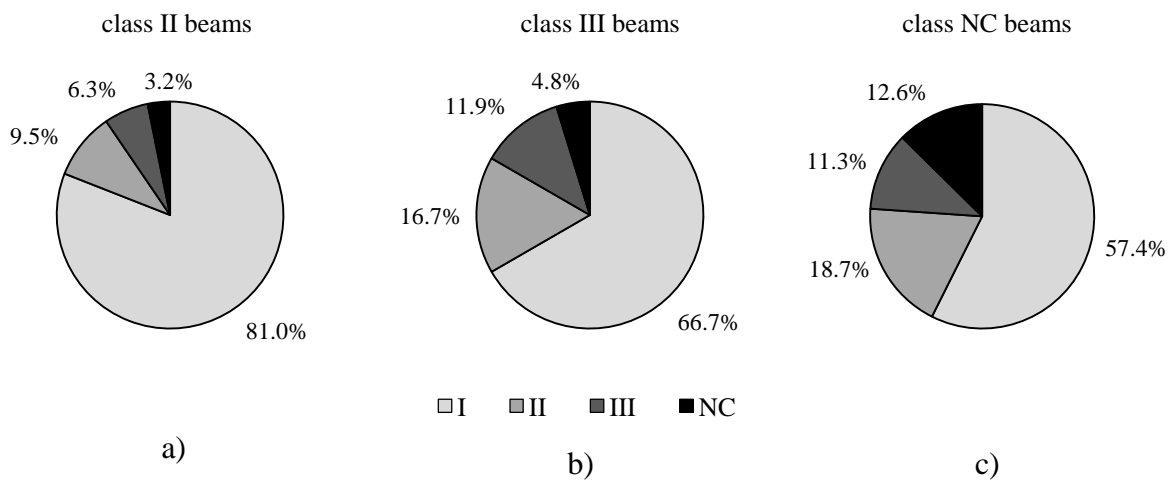


**Fig. 2** Distribution of boards visual grading for beams with different visual grade, as:  
a) class II; b) class III; c) class NC.

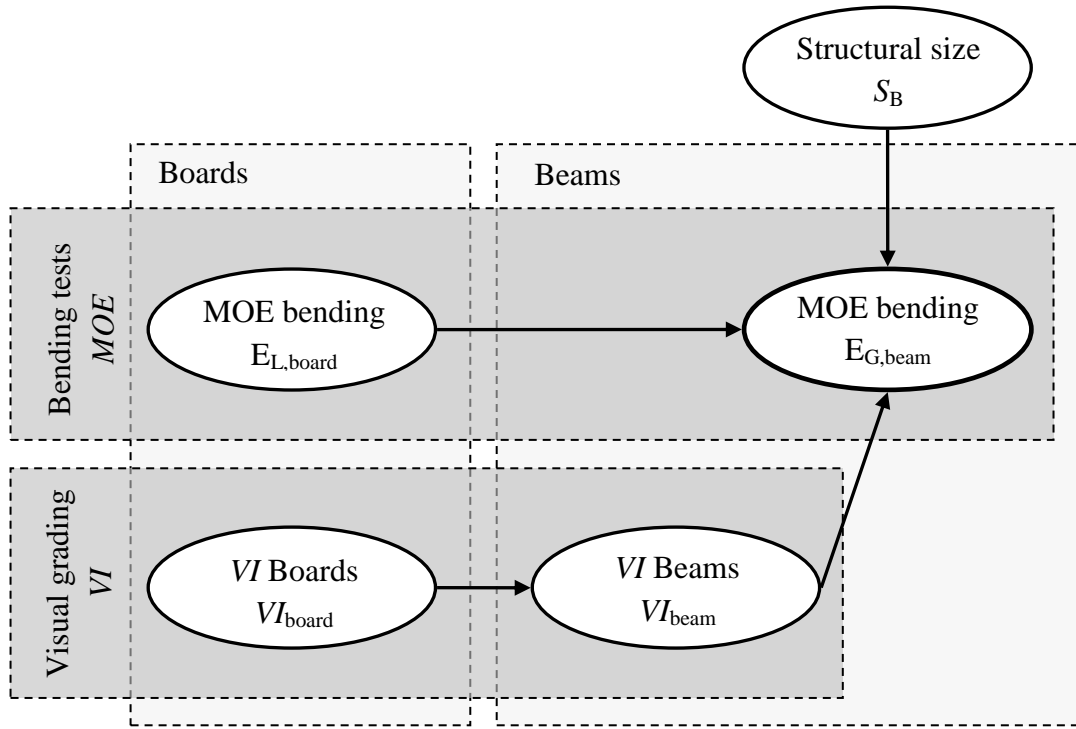


**Fig. 3** Hierarchical BPN to infer on global MOE in bending of structural size members by prior localized information in smaller size elements.

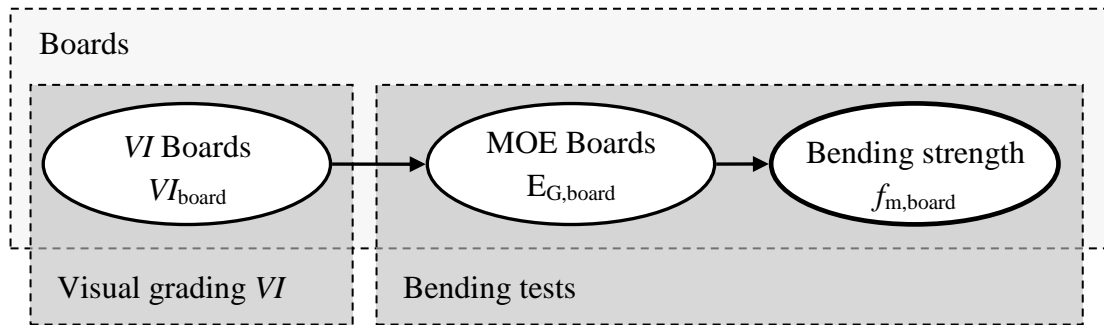


**Fig. 4** Simplified converging model.

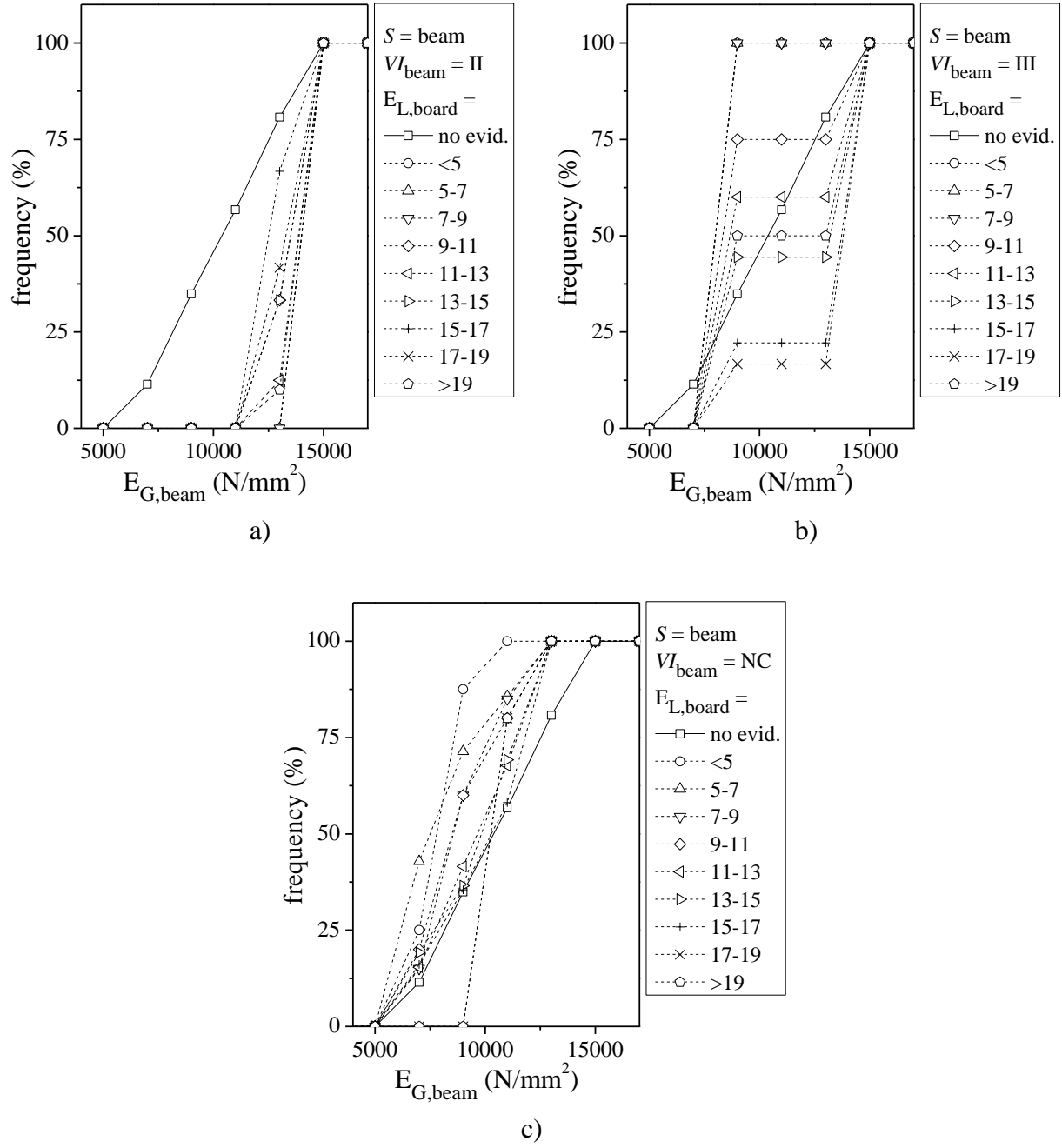


**Fig. 5** Cumulative frequency results for global MOE in bending for beams obtained with evidence in  $E_{L,board}$  results and beams' visual grade: a)  $VI_{beam} = II$ ; b)  $VI_{beam} = III$ ; c)  $VI_{beam} = NC$ . The markers indicate  $E_{L,board}$  results in kN/mm<sup>2</sup>.

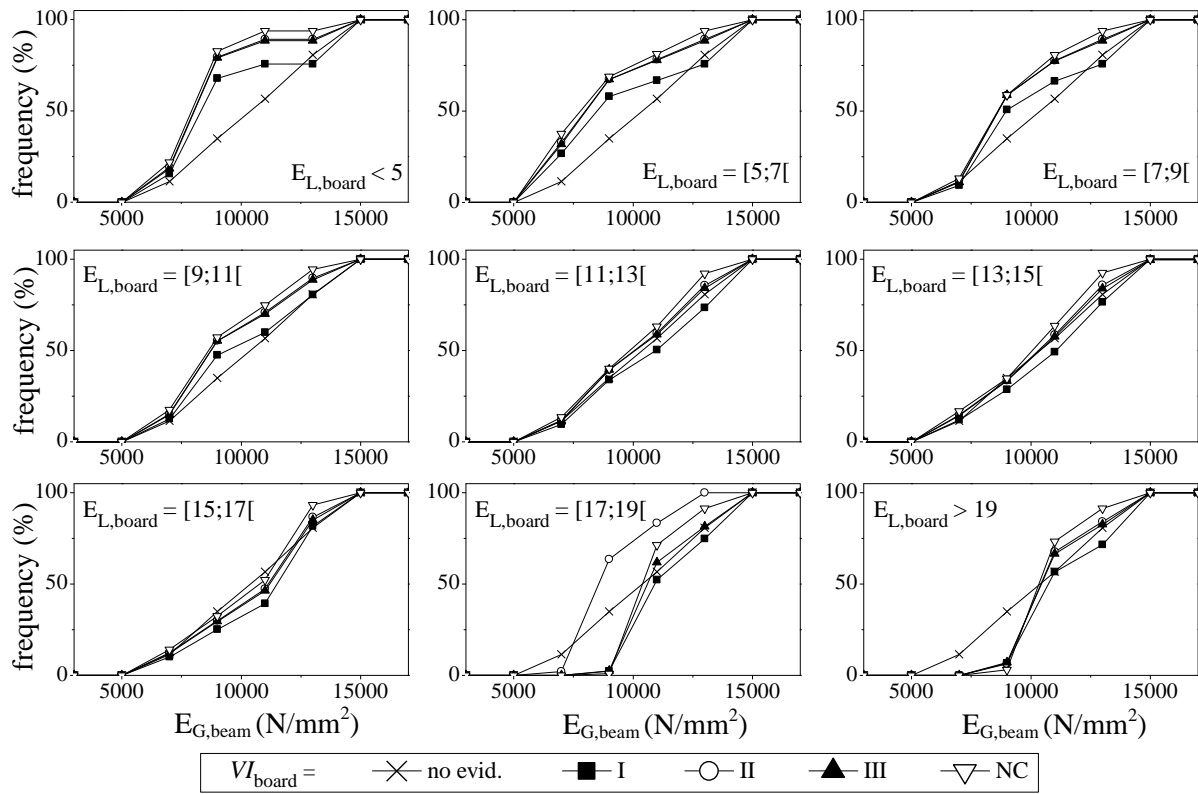


**Fig. 6** Evolution of cumulative frequency results with evidence in  $VI_{\text{board}}$ , throughout increasing of prior  $E_{L,\text{board}}$  (horizontal axes are  $E_{G,\text{beam}}$  in  $\text{N/mm}^2$  and vertical axes are frequency in %; the markers indicate  $E_{L,\text{board}}$  results in  $\text{kN/mm}^2$ ).

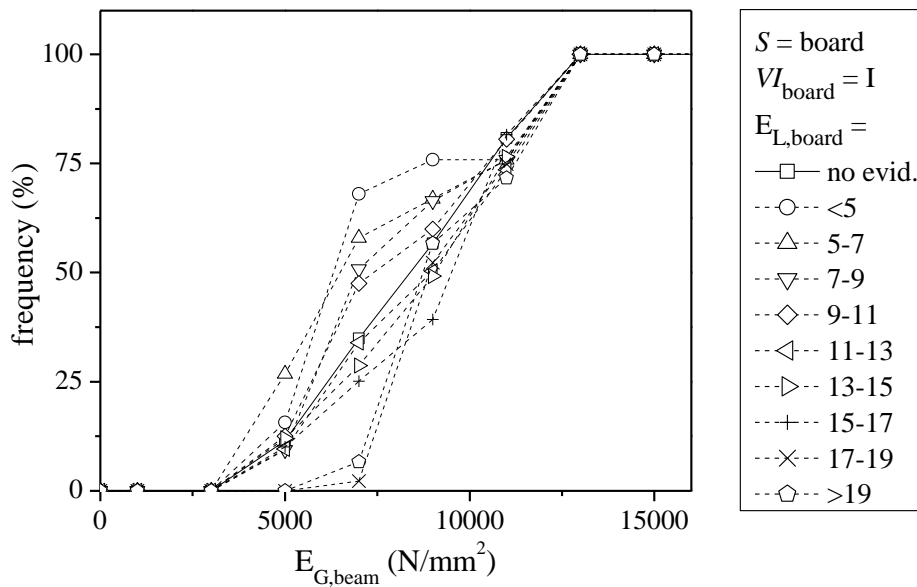


**Fig. 7** Cumulative frequency results for global MOE in bending for beams obtained with evidence in  $E_{L,\text{board}}$  results and for boards' visual grade I. The markers indicate  $E_{L,\text{board}}$  results in  $\text{kN/mm}^2$ .

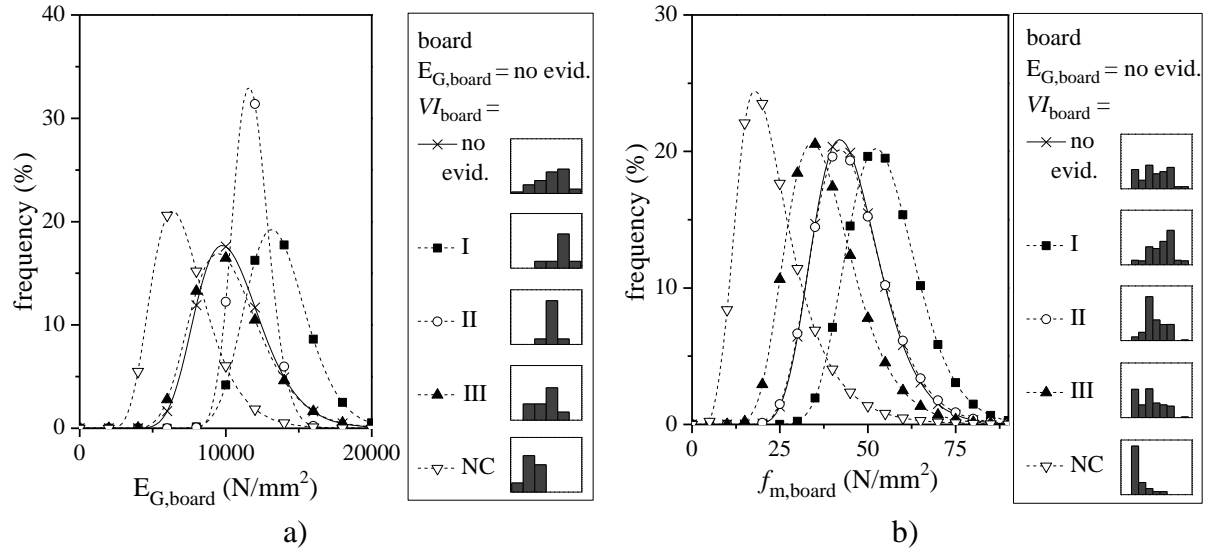


**Fig. 8** Histogram results in board scale, obtained with different evidences in  $VI_{board}$ , for a):  $E_{G,board}$ ; b)  $f_{m,board}$ . The markers indicate the  $VI_{board}$ .

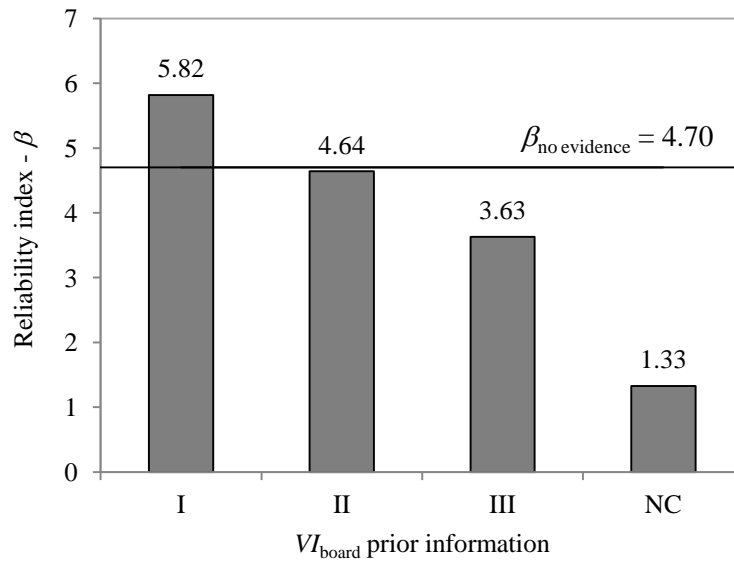


**Fig. 9** Reliability indices for different levels of prior information.



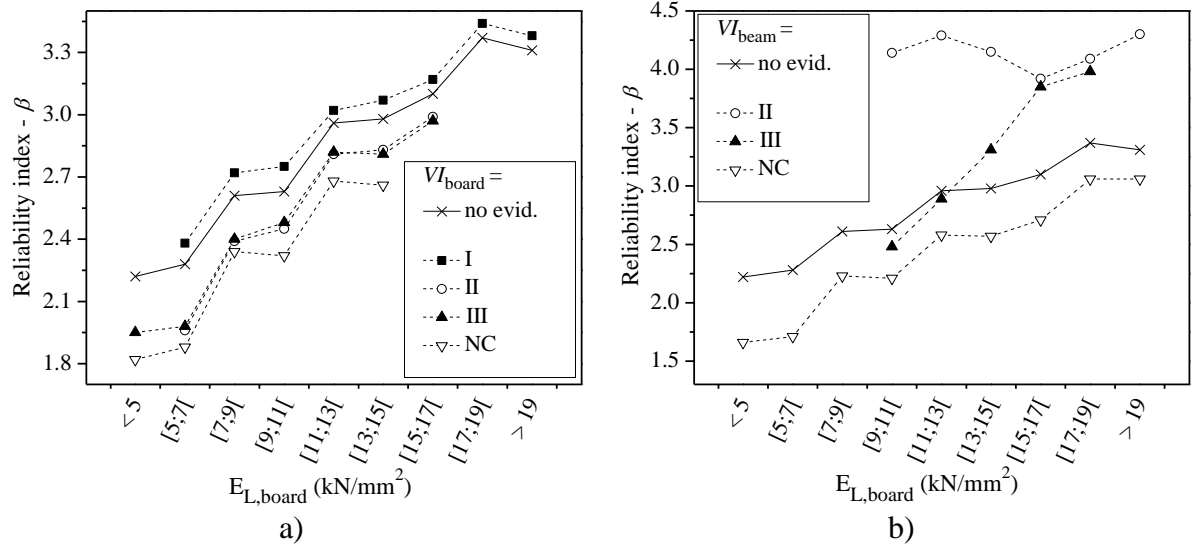


**Fig. 10** Reliability indices for different levels of prior information for the serviceability limit state with information in visual grade of: a) boards; b) beams.

## Tables:

**Table 1** Mean and coefficient of variation (CoV) values for bending stiffness and strength obtained from sawn beams and boards

Scale	Parameter	Visual grade	Mean (N/mm <sup>2</sup> )	CoV (%)	Sample size
Beam	$E_{L,beam}$	all	10840	25.3	20
		II	12590	25.3	5
		III	11480	16.5	2
		NC	10070	24.8	13
	$E_{G,beam}$	all	10940	22.0	20
		II	12630	21.3	5
		III	11380	35.4	2
		NC	10220	18.7	13
	$f_{m,beam}$	all	23.11	10.5	4
		II	24.16	3.0	2
		NC	22.05	16.2	2
Board	$E_{L,board}$	all	12910	30.4	336
		I	14030	25.4	211
		II	12600	25.7	56
		III	10720	34.9	35
		NC	8620	40.5	34
	$E_{G,board}$	all	11600	22.8	336
		I	12580	17.6	211
		II	11250	18.8	56
		III	10030	24.7	35
		NC	8210	30.1	34
	$f_{m,board}$	all	42.94	44.9	51
		I	57.30	22.7	24
		II	38.70	26.3	10
		III	33.06	45.4	9
		NC	16.26	35.8	8

**Table 2** Mean and characteristic values for different evidences in the BPN for infer on  $f_{m,board}$

Mechanical property		$VI_{board}$				
		no evid.	I	II	III	NC
$E_{G,board}$ (N/mm <sup>2</sup> )	mean (N/mm <sup>2</sup> )	10050	13120	11250	9860	6720
	CoV (%)	(23.8)	(16.1)	(10.5)	(25.7)	(31.3)
	5 <sup>th</sup> percentile (N/mm <sup>2</sup> )	6800	10070	9470	6460	4010
$f_{m,board}$ (N/mm <sup>2</sup> )	mean (N/mm <sup>2</sup> )	42.8	52.6	43.1	35.8	21.3
	CoV (%)	(23.6)	(19.4)	(24.4)	(29.6)	(49.9)
	5 <sup>th</sup> percentile (N/mm <sup>2</sup> )	29.1	38.2	28.9	22.0	9.4